Comparison of Battery Models for Energy Storage Applications on Insular Grids

E.M.G. Rodrigues, R. Godina, G.J. Osório, J.M. Lujano-Rojas, J.C.O. Matias, J.P.S. Catalão
University of Beira Interior, Covilhã, Portugal, and INESC-ID, IST, University of Lisbon, Lisbon, Portugal

***Abstract*—This paper explores different modelling techniques for representing electrochemical energy storage devices in insular power grid applications. Particular attention is given to Thevenin based and not Thevenin based models. A case study involving two insular power systems with renewable generation are used to stand out the performance of the selected battery technologies: Lithium-ion (Li-ion), Nickel–Cadmium (NiCd), Nickel–Metal Hydride (NiMH) and Lead Acid.**

Keywords—battery SOC; modelling techniques; insular grids; electrical energy storage; renewables integration.

I. INTRODUCTION

Wind and solar power resources are generally abundant in insular geographic regions. Nowadays, their exploration as source of electrical power in insular energy networks is common, even if their contribution to the present energy mix is reduced. The adoption of renewable sources at large scale in the grid is only meaningful if the intermittence of these sources is counterbalanced with additional sources of flexibility.

Energy Storage associated to renewable energy is fundamental for a transition to an efficient, reliable and cost effective power system free of carbon emissions [1]. Power grid energy storage refers to a number of different technologies with a wide range of characteristics. The available technologies can provide both power and energy related grid-services such as contingency, regulation and flexible reserves [2]. However not all show adequate performance when it comes to discharge times that cover short term and long term applications at same time [3].

A battery energy storage system (BESS) can be charged with the excess generated energy from wind power while filling the gaps between generation and supply during the rest of the operational period with a highly flexible capacity in terms of deploying full output power in a very short time or in a more extended period [4]. However to minimize the use of conventional energy by integrating renewable energy sources, it is necessary to evaluate the impact that a specific battery can have as well as the required sizes of the battery for demand-generation scenarios. Having that in mind a set of electrochemical batteries are modeled and compared using real demand/generation data provided under Singular project [5]. Two insular systems are analyzed: São Miguel and Crete Islands.

The Crete Island is the largest islanded power system in Greece and its electricity generation system is based generally on fossil fuels thermal power units. This island has a significant Renewable Energy Sources (RES) potential and it has been exploited during the past 16 years.

Over the last 3 years RES penetration remained steady around 20% and approximately 183MW of wind source. Also, 94MW of PV source has been already installed on the island [6].

The São Miguel Island is the major and most populated island in the Portuguese archipelago of the Azores. The island has approximately 140,000 inhabitants and covers 760 km². The electricity production and distribution provider Electricity of Azores (EDA) is focused on the importance of renewable energy, not only for environmental reasons, but also for reducing the islands' fossil fuel dependency [7]. It has 9MW of wind installed capacity which is translated in 6.35 % of the total power generation of São Miguel [8].

This paper is organized as follows: in Section II the battery electrical models are described. In section III the case study simulation results and critical analysis are presented and discussed. Finally, the conclusions are drawn in Section IV.

II. BATTERY MODELING THEORY

A. Electrical Modeling State of the Art

The working of a battery can be modeled in many ways, each method stressing on the specific operational features: electrochemical models, electrical models and mechanical models. Electrochemical models deal with the electrochemistry of the active species and their interaction with each other and with the membranes inside the cells of the battery. On the other hand electrical and mechanical models follow a black-box approach in analyzing the interaction of the battery with the system of which it is a part of. While mechanical models are more important to decide installation and operational safety for batteries, electrical models are inclined towards assessing the ability of integrating the battery as a part of electricity supply chain.

1) Electrochemical Model

The most common approach is based on Randles equivalent scheme. It consists of a serial resistance R_s that accounts for the ohmic voltage drops in the electrode and the electrolyte. The space charge which manifests at the electrode–electrolyte interface is represented by a capacitance C_{DL} called electric double layer capacitance.

This charge is generated by the difference of electrode and electrolyte internal potentials. The relationship is nonlinear given the low charge density in the electrolyte [9].

Another parameter modeled has to do with the electrode voltage at thermodynamic equilibrium designated as voltage source E_{th}.

978-1-4799-8725-2/15/$31.00 ©2015 IEEE

And finally an impedance term Z_F that describes the charge transfer effect at the electrode–electrolyte interface with the active material diffusion in electrode and electrolyte. The equations of electrochemistry which serve as a basis to calculate Randles parameters can be found in [10].

2) Thevenin Model

It is the most popular description since its representation is intuitive from electrical point view. The battery model takes a form of a voltage dc source in series with a resistance. In turn, charge transfer occurrences are associated with its own time constants leading to increased modeling complexity. To represent transient behavior correctly due to the electric double layer phenomenon, one or more RC networks can be included [11].

3) Advanced Thevenin Models

To create a more accurate behavior battery internal parameters must be formulated considering state of charge (SOC) dependency: open circuit voltage (OCV) as function of SOC, internal series resistance dependence on SOC or in the form of depth of discharge (DOD) [12]. An alternative approach determines battery voltage versus SOC through third order polynomial curves for various discharge currents [13]. Applying the same technique the polynomial description incorporates two RC parallel networks for short and longtime constants [14]. A model in which both storage capacitance and electrochemical resistance are approximated as continuous functions of OCV. Predicting charging behavior as well as discharging behavior can be found in [15]. As for parameters identification concerning Thevenin-based models, techniques can be divided into online identification [16] and on iterative numerical optimization (e.g. [17], [18]). Iterative identification tools employ genetic and nonlinear least squares estimation algorithms which require initial guesses. Normally the number of parameters to be estimated is high. The initial guesses for starting the identification process is the main drawback of these methods. In other words an incorrect guess may end up in a local minimum. Moreover, for an accurate identification the time spent on iterative simulations is also a disadvantage.

4) Zimmer Model

This model was created first for modeling NiCd battery. More recently other electrochemical battery types are under study considering this model [19]. The equivalent circuit comprises two RC networks. One describes the electrochemical energy storage while the other network models the diffusion phenomenon. In turn, each of RC networks parameters shows a dependence on temperature, SOC and current.

5) Harmonic Model

The electrochemical accumulator model is built through signal excitation to get a harmonic response. This is, a nonlinear equivalent circuit as function of load pulse frequency can be obtained by combining experimental impedance spectra along with a numerical identification method. Several works discuss this technique for Lead Acid batteries testing [16] and [20], NiMH batteries [21] or for modeling lithium-ion batteries [17]. As a matter of curiosity, the same modeling approach can be used to establish the electrical behavior concerning a proton exchange membrane fuel cell where the diffusion impedance is modeled by two RC cells [18].

The harmonic model approach fundamentally produces small signal models. This can be a limitation in large signal conditions because of electrochemical batteries nonlinearities. Then, it is difficult to obtain an equivalent circuit at a mean current different from zero due to the SOC dependence on battery behavior.

B. Modelling Theory

The method chosen for describing the NiMH, Li-ion and Lead Acid batteries response is based on Thevenin approach while the NiCd model is generated from the battery V-I data. The circuit element parameters used to build the respective models are described below.

1) NiCd

For this battery a classical Paatero model [20] is chosen. The battery voltage is described into two parts (open-circuit voltage U_{oc} and the overpotential U_{op}). The open-circuit voltage is defined as:

$$U_{oc} = a + b \times DOD + (c + d \times DOD) \times T \quad (1)$$

where T the battery temperature, DOD the depth of discharge while *a, b, c* and *d* are the model parameters to be fitted.

The overpotential U_{op} is determined as:

$$U_{op} = x_1 + x_2 \times T + x_3 \times DOD + x_4 \times |I| + \frac{x_5}{|I|} + (x_6 \times e^{x_7 DOD} + x_8) \times (e^{x_9 \times T} + x_{10}) \times |I| + x_{11} \times \tanh(x_{12} \times DOD + x_{12}) \quad (2)$$

where I is the battery current and x_i (i=1 to 10) are the model parameters that have to be calculated. Such values are giving in [20]. Then, total battery voltage can take the form:

$$U = U_{oc} - U_{op} \quad (3)$$

Battery capacity variation with the discharge current is modeled by:

$$C(I) = d_1 + e_1 \times I + f_1 \times arctang(g_1 + h_1 I) \quad (4)$$

where d_1, e_1, f_1, g_1 and h_1 are solved in order to fit the data published in [20]. Therefore, DOD calculation uses input data from battery current:

$$DOD(t) = \frac{1}{C(I)} \int_0^t I(t) \times dt \quad (5)$$

2) NiMH

The electric behavior can be described in accordance with the circuit diagram shown in Fig. 1. [22].

U_B, I_B are the terminal voltage and current, U_o is then open-cicuit voltage, R_i is the constant part of the internal resistance; R_D and C_D describe the effects on the surface of the electrodes (double layer capacity) while R_k and C_D describe diffusion processes in the electrolyte.

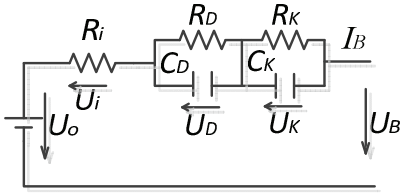

Fig. 1. NiMH battery model.

In the model is assumed that $\tau_D = R_D \times C_D$ and $\tau_K = R_K \times C_K$ represent short-time and long-term transient behavior respectively. Model parameters calculation needs only one current test pattern. R_i, R_D and C_D are extracted from the beginning of voltage response to a discharge pulse modeled by:

$$U(t) = U_i + U_D\left(1 - e^{-\left(\frac{t}{\tau_D}\right)}\right) + U_K\left(1 - e^{-\left(\frac{t}{\tau_k}\right)}\right) \quad (6)$$

To determine the relationship of NiMH battery SOC and electromotive force (EMF) a piecewise linearization strategy is adopted from [23].

$$SOC = \begin{cases} a_1 EMF + b_1 & EMF \rightarrow 0{\sim}0.1 \\ a_2 EMF + b_2 & EMF \rightarrow 0.1{\sim}0.8 \\ a_3 EMF + b_3 & EMF \rightarrow 0.8{\sim}1 \end{cases} \quad (7)$$

Consequently SOC dependency as function of battery current permits to describe the discharging regime as:

$$SOC = a_i U_t + a_i I_B(R_i + R_D + R_K) + a_i I_B R_D e^{\frac{-t}{\tau_D}} + a_i I_B R_K e^{\frac{-t}{\tau_K}} + b_i \quad (8)$$

As for charging regime follows as:

$$SOC = a_i U_t - a_i I_B(R_i + R_D + R_K) - a_i I_B R_D e^{\frac{-t}{\tau_D}} - a_i I_B R_K e^{\frac{-t}{\tau_K}} + b_i \quad (9)$$

3) Li-ion

As for electric circuit modeling for Li-ion batteries, [24] proposes the arrangement shown in Fig. 2, where E is the Li-ion battery's EMF, R_t internal resistance which includes all the resistances between electrodes, current collectors and electrode; $R_x C_x$ is the circuit time-constants, v_b is the terminal voltage whereas i_b is the battery current. R_t is found to be mainly dependent on the battery current. Thus the modeling equation has the form:

$$R_t = 2.4572 i_b^2 - 0.6101 i_b + 5.2497 \quad (10)$$

For the remaining parameters a two stage SOC dependency is modeled by two quadratic equations as:

$$R_s(SOC) = 72.42SOC^2 - 104.15SOC + 39.51,\ SOC > 52.5\% \quad (11)$$

$$R_s(SOC) = 96.57SOC^2 - 67.64SOC + 13.69,\ SOC \leq 52.5\% \quad (12)$$

$$R_m(SOC) = 48.98SOC^2 - 72.24SOC + 30.12,\ SOC > 57.5\% \quad (13)$$

$$R_m(SOC) = 23.28SOC^2 - 16.18SOC + 5.24,\ SOC \leq 57.5\% \quad (14)$$

$$R_f(SOC) = 11.76SOC^2 - 17.59SOC + 9.78,\ SOC > 57.5\% \quad (15)$$

$$R_f(SOC) = 1.41SOC^2 - 1.72SOC + 2.11,\ SOC \leq 57.5\% \quad (16)$$

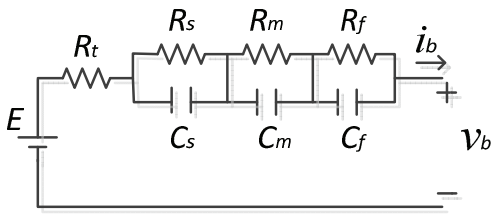

Fig. 2. Li-ion battery model.

Transient response is characterized by RC networks. Short and long time constants to a step load response are obtained as follows:

$$\tau_m(SOC) = \frac{1}{9.74SOC^2 - 14.01SOC + 6.09},\ SOC > 52.5\% \quad (17)$$

$$\tau_s(SOC) = \frac{1}{8.03SOC^2 - 5.15SOC + 1.91},\ SOC \leq 52.5\% \quad (18)$$

$$\tau_m(SOC) = \frac{1}{-20.94SOC^2 - 34.57SOC - 2.65}, SOC > 57.5\% \quad (19)$$

$$\tau_m(SOC) = \frac{1}{57.47SOC^2 - 56.42SOC + 23.74}, SOC \leq 57.5\% \quad (20)$$

$$\tau_f(SOC) = \frac{1}{240.43SOC^2 - 371.62SOC + 220.03}, SOC > 57.5\% \quad (21)$$

$$\tau_f(SOC) = \frac{1}{451.9SOC^2 - 383.26SOC + 156.8.03},\ SOC \leq 57.5 \quad (22)$$

Strong dependency of SOC on EMF requires experimental data by playing with different battery current levels. Such relation is shown in [25]. It is clear that a single curve fitting can describe a variety of battery current conditions.

Thus, battery voltage can be calculated combining the equations (23), (24) and (25) into equation (26).

$$U_{R_s||C_s}(t) = i_b R_s\left(1 - e^{\frac{-t}{\tau_s}}\right) + V_{sn0} e^{\frac{-t}{\tau_s}} \quad (23)$$

$$U_{R_m||C_m}(t) = i_b R_m\left(1 - e^{\frac{-t}{\tau_m}}\right) + V_{mn0} e^{\frac{-t}{\tau_m}} \quad (24)$$

$$U_{R_f||C_f}(t) = i_b R_f\left(1 - e^{\frac{-t}{\tau_f}}\right) + V_{fn0} e^{\frac{-t}{\tau_f}} \quad (25)$$

$$v_b(t) = E(t) - i_b R_t - U_{R_s||C_s}(t) - U_{R_m||C_m}(t) - U_{R_f||C_f}(t) \quad (26)$$

4) Lead Acid

An electric network for modeling Lead Acid type battery can be built using one series resistance R and a single RC block for short time behavior. However when operating at low charge/discharge, an additional RC block provides better accuracy [26]. A further improvement of the model can be achieved considering a parasitic branch which models the irreversible reactions that take place due to the electrolysis of water at the ending of charging process. Therefore, the parasitic branch draw some of battery current that does not contribute for charging the battery. The equivalent electric network model is shown in Fig 3. [27] where E_m is the EMF, R_o is the polarization resistance, $R_1 C_1$ is the short term transient response, $R_2 C_2$ is the long term response and $I(V_{PN})$ is the parasitic branch current.

In this model the elements of this circuit do not depend constantly on the battery SOC and on electrolyte temperature. However it is assumed time constants τ_1 and τ_2 are constant.

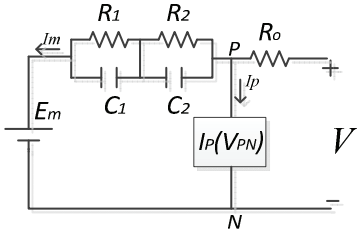

Fig. 3. Lead Acid battery equivalent network

Equation (27) determines open circuit voltage as function of SOC and electrolyte temperature (θ).

$$E_m = E_{m0} - K_E(273 + \theta)(1 - SOC) \quad (27)$$

As for the internal parasite resistances the temperature has no influence only affected by SOC.

$$R_o = R_{00}[1 + A_o(1 - SOC)] \quad (28)$$

$$R_1 = -R_{10}\ln(SOC) \quad (29)$$

$$R_2 = R_{20}\frac{\exp[A_{21}(1-SOC)]}{1+\exp(\frac{A_{22}I_m}{I^*})} \quad (30)$$

where E_m, K_E, R_{00}, A_o, R_{10}, R_{20}, A_{21}, A_{22}, are constants obtained from battery experimental tests.

Since the behavior of the parasitc branch is strongly non-linear it is approximated by the Tafel gassing current relationship [28]:

$$I_P = V_{PN}G_{po}\exp\left(\frac{V_{PN}}{V_{po}+A_p\left(\frac{1-\theta}{\theta_f}\right)}\right) \quad (31)$$

where G_{po} , V_{po}, A_p are constants estimated by experimental procedures and θ_f is the electrolyte freezing temperature.

III. Case Study

Two insular power systems are simulated in order to test and evaluate energy storage sizing based on four battery models. To provide meaningful outcomes real data concerning São Miguel and Crete Islands are used. Both grids are different in terms of size, configuration and conventional installed power capacity as well renewable power plants connected to the system. Meaning that, the ratio renewable resources vs total installed power generation is considerable lower for S. Miguel when compared to Crete Island.

The models are aggregated in cell banks replicating a storage system that must respond to the demands of the grid. Therefore, the operation strategy works by charging the battery with excess generated energy at times of low demand in order to be discharged to the grid later when needed at ON peak hours.

A week of data was utilized for this study. A data sample from S. Miguel renewable resources is shown in Fig. 4.

Basic Battery Specifications for Modeling Parameters are shown in Table 1 [25] [29].

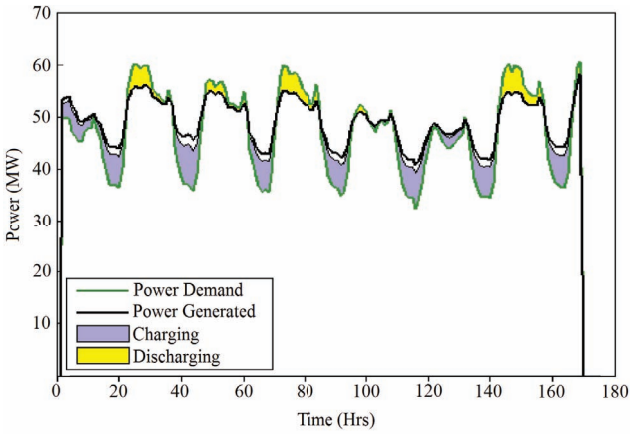

Fig. 4. Data sample from S. Miguel renewable resources

Each BESS type is evaluated using two merit figures: Storage capability (SC) and Demand Capability (DC) which assess the percentage of excess power charging to and discharging from the battery.

$$SC = \frac{Total\ Charged}{Total\ Generated - Total\ Bypassed} \quad (32)$$

$$DC = \frac{Total\ Discharged}{Total\ Demand - Total\ Bypassed} \quad (33)$$

A. Sizing based on a fixed number of cells

To assess the capability of different battery types for large-scale energy storage each model are executed using the same initial parameters but adjusting the battery type variable in each case. BESS SOC is initially set at 30%. In this test each BESS is designed with 400 identical cells. Results are shown in Tables II.

These capability indicators obtained show how the low charge and discharge rates of the Lead Acid battery greatly reduce its performance, meaning it will not efficiently make use of the generated power to meet demand.

The battery with the lowest cyclic performance reduction and thus longest life is the NiCd, this also has the highest storage and demand capability (the only type to supply 100% demand).

NiCd also produces a high final SOC, meaning that the battery is 'self-sufficient' within the time period so is less likely to need an occasional 'booster' charge from an external source. Assessing the final SOC is not, however, a practical method for measuring battery performances as it will be offset by the periods of time at which the battery is at maximum or minimum capacity.

TABLE I. Variable Properties of Different Available Battery Types

Type	Cycles (80%)	Charge Time (h)	Discharge Month (%)	Cost ($/ KWh)	Voltage (V)	Peak Drain (C)	Specific Energy (W h/kg)	Specific Power (W/kg)	Rated Capacity mAh
Li-ion	500-1000	2-4	10	24	4.2	2	90-190	500-2000	5300
NiMH	300-500	2-4	30	18.5	1.25	5	45-80	200-1500	2300
NiCd	1500	1	20	7.5	1.25	20	40-65	100-175	2800
Lead Acid	200-2000	8-16	5	8.5	2	5	20-40	75-415	2000

TABLE II. BESS PERFORMANCE COMPARISON

Battery	Initial SOC	Final SOC	Azores SC	Azores DC	Crete Final SOC	Crete SC	Crete SD
Li-ion	30	33.93	91.56	96.54	909.895	109.900	184.498
NiMH	30	32.98	86.43	96.54	933.947	159.468	184.498
NiCd	30	33.85	94.82	100	956.316	217.343	452.083
Lead Acid	30	29.45	26.83	80.81	842.722	360.337	129.024

B. Sizing as function of variable number of cells

The comparison of performances concerning S. Miguel Island of these batteries is shown in Fig. 5 and 6. As can be seen in both scenarios the storage capability indicator increases with the number of cells until a limit is reached.

As to demand capability performance the NiCd battery is the only battery type which can maintain 100% demand capability, though NiMH and Li-ion are very close. The equivalent simulations related to Crete Island are show in Fig. 7. and Fig. 8. The Lead Acid battery is appearing to be for this study as the least suitable for both power grids. To maintain demand capability with any battery other than Lead Acid the number of cells could be as low as 5. To make efficient use of the storage capacity and maintain as much generated energy as possible a suitable number of cells would be 30 (S. Miguel). For larger systems the required number of cells might need to increase that is the case of Crete Island, which requires a much larger size and approximately 1600 cells would be needed.

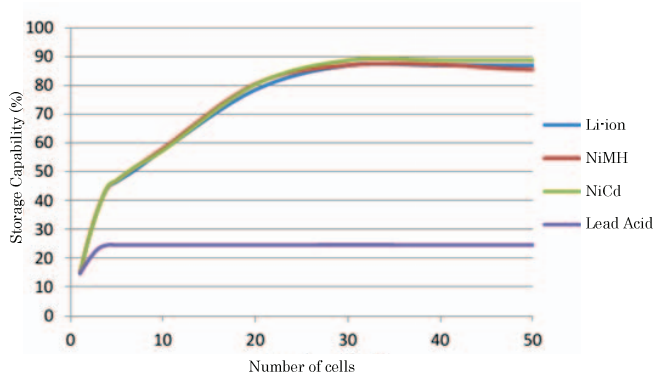

Fig. 5. S. Miguel Island: Storage Capability

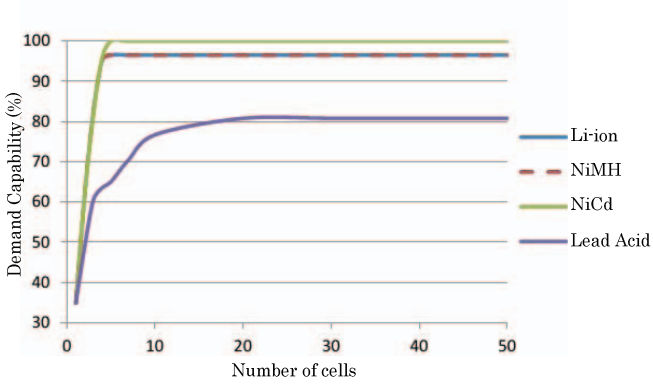

Fig. 6 S. Miguel Island: Demand Capability.

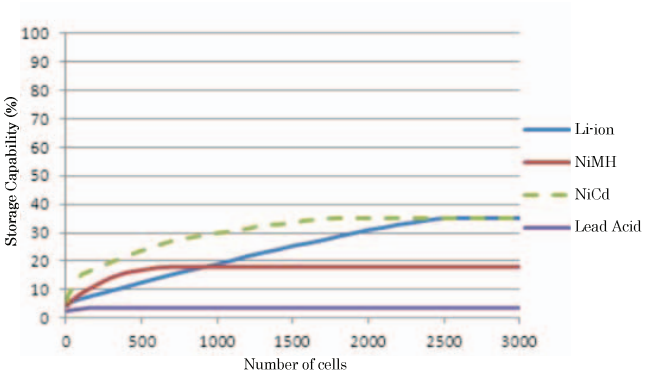

Fig. 7. Crete Island: Storage capability.

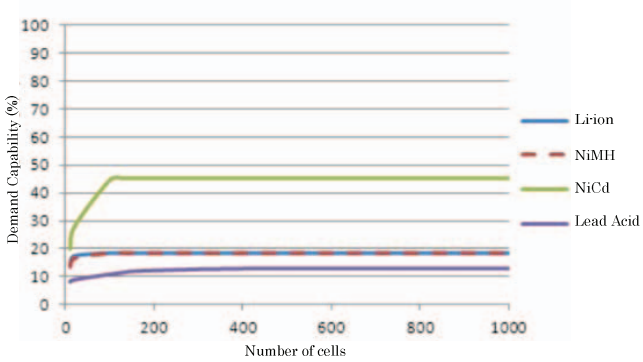

Fig. 8. Crete Island: Demand capability.

Despite performing better, NiCd batteries have to be handled with caution since they display weaknesses such as nickel and cadmium being toxic heavy metals which results in environmental threats and also suffering from memory effect – the maximum capacity can be radically decreased if the battery is frequently recharged after being only partly discharged [29]. Proper battery management systems need to be implemented in order to mitigate this effect.

C. Sizing as function of number of string

By determining the required number of cells the number of parallel strings can also be analyzed. For the S. Miguel system with low charge rates and only 30 cells there is a limit to the number of strings which can be chosen. Fig. 9 presents DC indicator outcome for both power systems exploring the arrangement based on parallel strings.

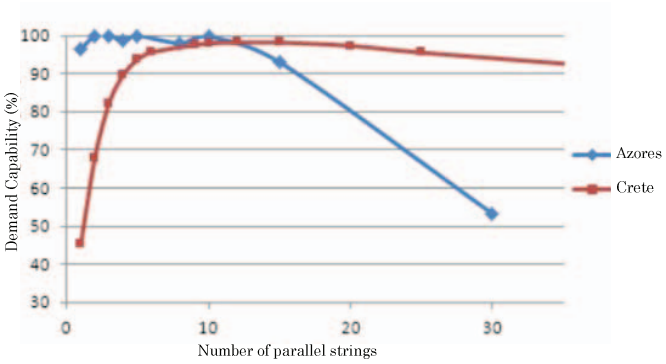

Fig. 9. Demand capability vs number of strings.

Reporting to Azores (Li-ion battery) the optimal arrangement is the cell format 10S3P (3 parallel strings of 10 cells in series). For the case of Crete and the present study the most suited battery is NiCd – 1800 cells. Using parallel strings the optimal value is found in 120S15P with 98.17% demand capability. It can be seen that if a high charge rate is required the demand capability will improve with the number of strings. The storage capability size vs number of strings can be observed in Fig. 10.

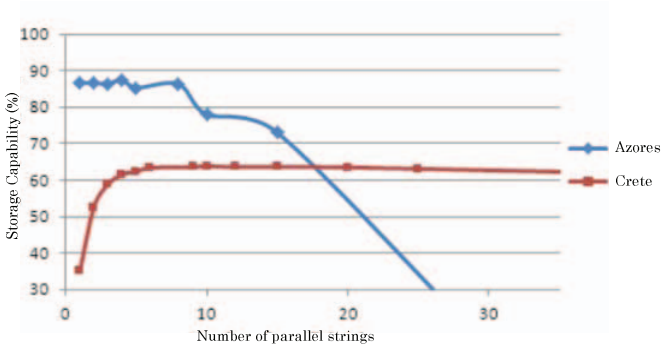

Fig. 10. Storage capability vs number of strings.

IV. Conclusion

This paper has addressed energy storage performance of four electrochemical battery models (Li-ion, NiCd, NiMH and Lead Acid) to support grid demand with surplus wind power. The insular systems of S. Miguel and Crete islands served as study basis and, as a result, NiCd battery presented the best performance in storage and demand capability. S. Miguel Island, being a small power system only requires a sizing made up of 30 battery cells. For larger systems such as Crete Island, a much larger battery of approximately 1600 cells would be required. Li-ion follows closely to NiCd except when assessing Crete Island's demand capability. NiCd batteries seem to be the best choice to support the grid, but since these batteries suffer from memory effect, battery management solutions have to be designed carefully. Granting that the islands contrast in size, a cost-benefit analysis needs to be conducted in order to assess if the choice found in this paper fits both islands.

Acknowledgment

This work was supported by FEDER funds through COMPETE and by Portuguese funds through FCT, under FCOMP-01-0124-FEDER-020282 (Ref. PTDC/EEA-EEL/118519/2010), UID/CEC/50021/2013 and SFRH/BPD/103079/2014, and also by funds from the EU 7th Framework Programme FP7/2007-2013 under GA no. 309048.

References

[1] M. Hozouri, A. Abbaspour, M. Fotuhi-Firuzabad and M. Moeini-Aghtaie, "On the Use of Pumped Storage for Wind Energy Maximization in Transmission-Constrained Power Systems," *IEEE Transactions on Power Systems,* vol. 30, no. 2, pp. 1017-1025, 2015.

[2] P. Denholm, J. Jorgenson, M. Hummon, T. Jenkin and D. Palchak, "The Value of Energy Storage for Grid Applications," National Renewable Energy Laboratory, Denver, 2013.

[3] E. Rodrigues, A. Bizuayehu and J. P. Catalao, "Analysis of requirements in insular grid codes for large-scale integration of renewable generation," in *2014 IEEE PES T&D Conference and Exposition*, Chicago, IL, USA, 2014.

[4] F. Luo, K. Meng, Z. Y. Dong, Y. Zheng, Y. Chen and K. P. Wong, "Coordinated Operational Planning for Wind Farm With Battery Energy Storage System," *IEEE Transactions on Sustainable Energy,* vol. 6, no. 1, pp. 253-262, 2015.

[5] SiNGULAR, "Smart and Sustainable Insular Electricity Grids Under Large-Scale Renewable Integration," Grant Agreement No: 309048, FP7-EU, 2015. [Online]. Available: http://www.singular-fp7.eu/home/. [Accessed 2015].

[6] T. Tsoutsos, I. Tsitoura, D. Kokologos and K. Kalaitzakis, "Sustainable siting process in large wind farms case study in Crete," *Renewable Energy,* vol. 75, pp. 474-480, 2015.

[7] C. Camus and T. Farias, "The electric vehicles as a mean to reduce CO2 emissions and energy costs in isolated regions. The São Miguel (Azores) case study," *Energy Policy,* vol. 43, p. 153–165, 2012.

[8] EDA S.A. - Electricidade dos Açores, "Caracterização Das Redes De Transporte E Distribuição De Energia Eléctrica Da Região Autónoma Dos Açores," Ponta Delgada, 2014.

[9] B. E. Conway, Electrochemical supercapacitors: scientific fundamentals and technological applications, New York: Springer, 2009.

[10] A. Jossen, "Fundamentals of battery dynamics," *Journal of Power Sources,* vol. 154, no. 2, pp. 530-538, 2006.

[11] H. Chan, "A new battery model for use with battery energy storage systems and electric vehicles power systems," in *IEEE Power Engineering Society Winter Meeting, 2000.*, 2000.

[12] M. G. Jayne and C. Morgan, "The modelling a lead acid batteries for electric vehicle applications," in *32nd International Power Sources Symposium*, Cherry HilL, 1986.

[13] I. Papic, "Simulation model for discharging a lead-acid battery energy storage system for load leveling," *IEEE Transactions on Energy Conversion,* vol. 21, no. 2, pp. 608-615, 2006.

[14] M. Chen and G. Rincon-Mora, "Accurate electrical battery model capable of predicting runtime and I-V performance," *IEEE Transactions on Energy Conversion,* vol. 21, no. 2, pp. 504-511, 2006.

[15] Z. Salameh, M. Casacca and W. A. Lynch, "A mathematical model for lead-acid batteries," *IEEE Transactions on Energy Conversion,* vol. 7, no. 1, pp. 93-98, 1992.

[16] O. Bohlen, S. Buller, R. De Doncker, M. Gelbke and R. Naumann, "Impedance based battery diagnosis for automotive applications," in *IEEE 35th Annual Power Electronics Specialists Conference, 2004.*, Aachen, Germany, 2004.

[17] S. Buller, M. Thele, R. De Doncker and E. Karden, "Impedance-based simulation models of supercapacitors and Li-ion batteries for power electronic applications," in *38th IAS Annual Meeting. Conference Record of the Industry Applications Conference, 2003.*, 2003.

[18] P. T. J.-P. M. S. R. B. D. I. Sadli, "Behaviour of a PEMFC supplying a low voltage static converter," *Journal of Power Sources,* vol. 156, no. 1, pp. 119-125, 2006.

[19] D. Fan and R. E. White, "A Mathematical Model of a Sealed Nickel-Cadmium Battery," *Journal of the Electrochemical Society,* vol. 138, no. 1, pp. 17-25, 1991.

[20] G. Sperandio, C. Nascimento and G. Adabo, "Modeling and simulation of nickel-cadmium batteries during discharge," in *2011 IEEE Aerospace Conference*, Big Sky, MT, 2011.

[21] E. Kuhn, C. Forgez, P. Lagonotte and G. Friedrich, "Modelling Ni-mH battery using Cauer and Foster structures," *Journal of Power Sources,* vol. 158, no. 2, pp. 1490-1497, 2006.

[22] B. Schweighofer, K. Raab and G. Brasseur, "Modeling of high power automotive batteries by the use of an automated test system," *IEEE Transactions on Instrumentation and Measurement,* vol. 52, no. 4, pp. 1087-1091, 2003.

[23] W. Guoliang, L. Rengui, Z. Chunbo and C. C.C., "State of charge Estimation for NiMH Battery based on electromotive force method," in *2008. VPPC '08. IEEE Vehicle Power and Propulsion Conference*, Harbin, 2008.

[24] Y.-C. Hsieh, T.-D. Lin, R.-J. Chen and H.-Y. Lin, "Electric circuit modelling for lithium-ion batteries by intermittent discharging," *IET Power Electronics,* vol. 7, no. 10, pp. 2672-2677, 2014.

[25] P. D. Lund, J. Lindgren, J. Mikkola and J. Salpakari, "Review of energy system flexibility measures to enable high levels of variable renewable electricity," *Renewable and Sustainable Energy Reviews,* vol. 45, pp. 785-807, 2015.

[26] C.-J. Zhan, X. Wu, S. Kromlidis, V. Ramachandaramurthy, M. Barnes, N. Jenkins and A. Ruddell, "Two electrical models of the lead-acid battery used in a dynamic voltage restorer," *IEE Proceedings on Generation, Transmission and Distribution,* vol. 150, no. 2, pp. 175-182, 2003.

[27] M. Ceraolo, "New dynamical models of lead-acid batteries," *IEEE Transactions on Power Systems,* vol. 15, no. 4, pp. 1184-1190, 2000.

[28] S. Barsali and M. Ceraolo, "Dynamical Models of Lead-Acid Batteries: Implementation Issues," *IEEE Transactions on Energy Conversion,* vol. 17, no. 1, pp. 16-23, 2002.

[29] X. Luo, J. Wang, M. Dooner and J. Clarke, "Overview of current development in electrical energy storage technologies and the application potential in power system operation," *Applied Energy,* vol. 137, pp. 511-536, 2015.